Methane Activation with Rhenium Catalysts. 1. Bidentate Oxygenated Ligands

Jason M. Gonzales,[†] Jonas Oxgaard,[†] Roy A. Periana,[‡] and William A. Goddard III*,[†]

Materials and Process Simulation Center (139-74), California Institute of Technology, Pasadena, California 91125, and Donald P. and Katherine B. Loker Hydrocarbon Research Institute and Department of Chemistry, University of Southern California, Los Angeles, California 90089

Trends in methane activation have been explored for rhenium-based catalysts in conjunction with bidentate oxygenated ligands of the form $(L_1)(L_2)Re(OH)(OH_2)$ [L_1, L_2 = acac, catechol, glycol]. When placed in acidic media, the equilibrium for this reference catalyst shifts to the protonated forms $(L_1)(L_2)Re(OH_2)(OH_2)$ in almost all cases. In all cases the activation of the reference complex proceeds through a concerted metathesis type transition state, and only one of the 13 reference complexes proceeds with methane activation through a barrier of less than 35 kcal mol^{-1}. Study of the identity complexes (L_1 = L_2) revealed that protonation of the ligand oxygens is unfavorable for acac and catechol, but favorable for glycol; however in only one case is the barrier for methane activation improved by this route. Electron density on the central rhenium is the best predictor for the magnitude of the methane activation barrier; namely, increased electron density (obtained by considering lower oxidation states) on the metal leads to lower barriers. Lower oxidation states form weaker Re−O bonds, which increase lability of the leaving groups and decrease the barrier to proton transfer from methane.

Introduction

The conversion of methane to a more functionalized form is an important topic in homogeneous catalysis. While methane is a very efficient fuel, its gaseous nature makes transportation difficult, and numerous scientists have tackled the problem of methane activation and functionalization, mainly through the use of transition metal-based catalysts.[1−5] Recent studies with methyl rhenium trioxide[6] by our group showed novel nonredox metal−carbon functionalization and led us to an interest in exploring methane activation with oxygenated ligands. However, we do not currently have a set of promising rhenium-based catalysts for methane activation, nor do we understand the systematic trends for these types of ligands linked to rhenium. The current work is an effort to ameliorate this problem for oxygenated bidentate ligands.

In the experimental world, particularly the pharmaceutical industry, combinatorial chemistry is used to develop insight into large libraries of chemical compounds.[7−9] In principle this process could be used to take a large set of potential catalysts and screen a subset that show reactivity beyond a certain threshold for more detailed analysis. Quantum mechanical rapid prototyping (QMRP) is the computational analogue to combinatorial chemistry. Designed by Muller and Goddard,[10] it is a strategy for simplifying the exhaustive work necessary to characterize catalytic cycles for large numbers of possible metal/ligand combinations for methane activation, the idea being to isolate a set of screening criteria that can be used to quickly analyze potential ligands and discard nonviable candidates with a minimum of computational effort.

Scheme 1 highlights the methane activation reactions that can proceed from the reference molecule $(L_1)(L_2)Re(OH)(OH_2)$. The methane itself can react in three ways: in a concerted reaction via metathesis, by way of explicit oxidative addition and concomitant reductive elimination, and finally through the oxidative hydrogen migration (OHM) mechanism of Oxgaard et al.[11] When QMRP is applied to methane activation, two initial criteria are applied to separate catalysts: (1) the *thermodynamic criterion*, which requires the relative enthalpy of the activated intermediate to be less than 10 kcal mol^{-1} above the reference (i.e., the relative enthalpy of species **4** is less than 10 kcal mol^{-1}), and (2) the *kinetic criterion*, which necessitates that the barrier to methane activation lie below 35 kcal mol^{-1} (i.e., the relative enthalpy of either species **3** or the higher of species **5** and **7** is less than 35 kcal mol^{-1}).

In its usual incarnation QMRP is merely a screening protocol, in which the goal is a set of potentially active catalysts for further study. As such, we would not compute transition states for species that do not satisfy the first criterion. However, during the preliminary portion of the current investigation of oxygenated rhenium systems, we realized that the data obtained from earlier QMRP work could easily be extended to a more complete survey to understand trends between ligands and reactivity. It should be noted that we did not map out full mechanistic pathways for these reactions, only representative intermediates

* Corresponding author. E-mail: wag@wag.caltech.edu.
† California Institute of Technology.
‡ University of Southern California.
(1) Crabtree, R. H. *Chem. Rev.* **1995**, *95*, 987.
(2) Shilov, A. E.; Shul'pin, G. B. *Chem. Rev.* **1997**, *97*, 2879.
(3) Oxgaard, J.; Periana, R. A.; Goddard, W. A., III. *J. Am. Chem. Soc.* **2004**, *126*, 11658.
(4) Wang, G. J.; Gong, Y.; Chen, M. H.; Zhou, M. F. *J. Am. Chem. Soc.* **2006**, *128* (5974).
(5) Owen, J. S.; Labinger, J. A.; Bercaw, J. E. *J. Am. Chem. Soc.* **2006**, *128*, 2005.
(6) Conley, B. L.; Gonzales, J. M.; Ganesh, S. K.; Tenn, W. J., III; Young, K. J. H.; Oxgaard, J.; Goddard, W. A., III; Periana, R. A. *J. Am. Chem. Soc.* **2006**, *128*, 9018.
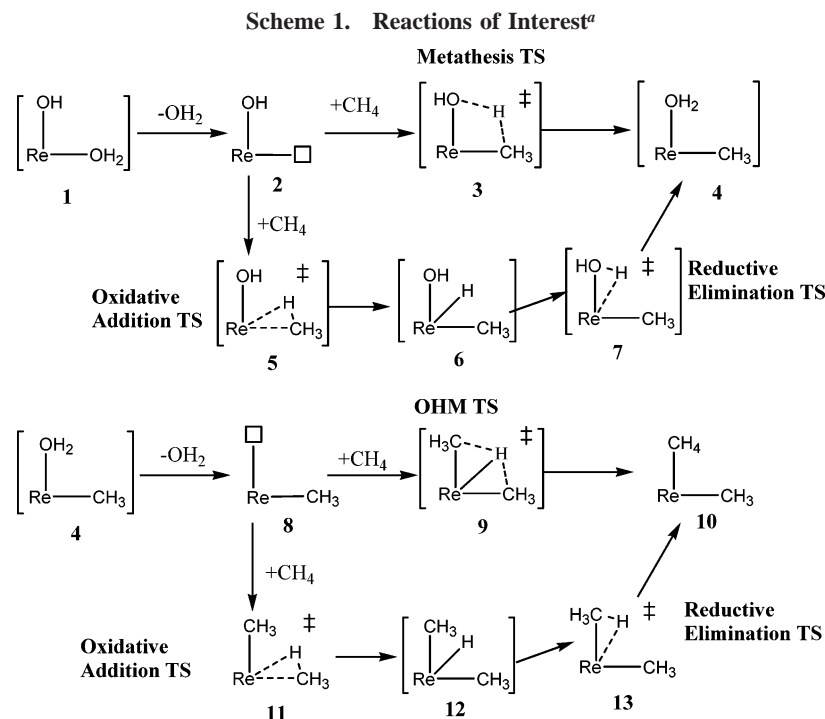(7) Thompson, L. A.; Ellman, J. A. *Chem. Rev.* **1996**, *96*, 555.
(8) Kassel, D. B. *Chem. Rev.* **2001**, *101*, 255.
(9) Nicolaou, K. C.; Hanko, R.; Hartwig, W. *Handbook of Combinatorial Chemistry: Drugs, Catalysts, Materials*; Wiley-VCH: New York, 2002.

(10) Muller, R. P.; Phillip, D. M.; Goddard, W. A., III. *Top. Catal.* **2003**, *23*, 81.
(11) Oxgaard, J.; Muller, R. P.; Goddard, W. A., III; Periana, R. A. *J. Am. Chem. Soc.* **2004**, *126*, 352.

Scheme 1.   Reactions of Interest[a]

Metathesis TS

1   2   3   4

Oxidative Addition TS   5   6   7   Reductive Elimination TS

OHM TS

4   8   9   10

Oxidative Addition TS   11   12   13   Reductive Elimination TS

[a] Only the species in brackets were computed. The assumed ligands L_1 and L_2 are not shown for clarity.
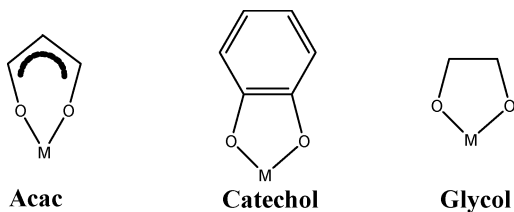
Figure 1. Ligands utilized in the present study.

Acac   Catechol   Glycol

cis to both acac oxygens

Acac   Higher alphabetically   OH_2

Glycol

Acac   *trans* to one of the acac oxygens   OH

Glycol

Figure 2. Characterization of *cis* and *trans* reference structures for acac and glycol.

and transition states. Thus, for example, weakly bound complexes of the type $(L_1)(L_2)Re(OH)(CH_4)$ were not computed. While it is possible that the formation of the agostic species could be the rate-determining step for a particular C−H activation reaction, we elected to limit full mechanistic mapping to systems that fulfill the two criteria outlined above.

Note that in Scheme 1 no OHM type transition state to form **4** is listed, as we were unable to find such a mechanism. However, the second activation of $(L_1)(L_2)Re(OH_2)(CH_3)$ proceeds through an OHM mechanism and/or a conventional oxidative addition/reductive elimination (in contradiction to our prior work postulating that oxidative addition and oxidative hydrogen migration were mutually exclusive[3,11]), while no metathesis type transition state was found.

While the number of potential rhenium ligands is vast, in this first report we restrict ourselves to oxygenated bidentate ligands, as listed in Figure 1. Our design criteria follow several restrictions: (1) only the ground states of oxidation states III and V, as we believe that Re(I) would be too unstable to catalytic conditions, while Re(VII) would be too inert to methane; (2) only coordinately saturated complexes, as we believe unsaturated species would not survive the experimental conditions; (3) only oxygenated ligands in this first exploration, although this is currently being expanded; (4) only chelating ligands, as we believe this imparts improved stability on the eventual catalyst, while simultaneously decreasing the complexity of the computational effort.

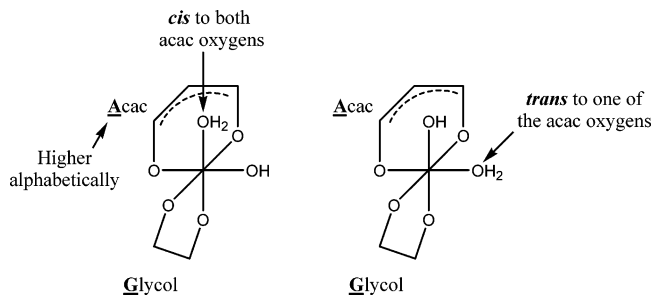Thus, we have included several possible combinations of ligands to form $(L_1)(L_2)Re(OH)(OH_2)$: acac, catechol, and glycol, which we will note as the reference complex. The set is meant to be representative of different types of bidentate oxygen linkages, forming species in oxidation states of Re(III) and Re(V). We will also consider the asymmetric cases $L_1 \neq L_2$. In this case there are *cis* and *trans* isomers. Our naming scheme is illustrated by our reference molecule $L_1L_2Re(OH)(OH_2)$, where the species that has the earlier alphabetical L_1 with both of the linkage atoms *cis* to OH_2 is the *cis* case. Figure 2 shows the *cis*/*trans* cases for (acac)(glycol)Re(OH)(OH_2). All species that are made from *cis* $(L_1)(L_2)Re(OH)(OH_2)$ are labeled *cis*, even if a water is placed in another location.

In addition to the conventionally bound species we will consider several different types of protonated species for the $L_1 = L_2$ identity cases. This will include studying the effects of single protonation of oxygens *cis* and *trans* to the reference water in $(L)_2Re(OH)(OH_2)$ as well as double protonation of the ligand with an oxygen *trans* to the reference water and double cross-protonation of two *cis* oxygens (see Figure 3 for a pictographic description). Careful note should be made to recognize that the *cis* and *trans* shown in Figure 3 are distinct from the *cis* and *trans* shown in Figure 2. Here it refers to the location of the additional proton placed on the L ligand with respect to the OH/OH_2 in the reference molecule, while in the former case describes the orientation of the L ligands themselves.

The goal of the present work is to analyze the trends of the many reactions considered here as a function of several
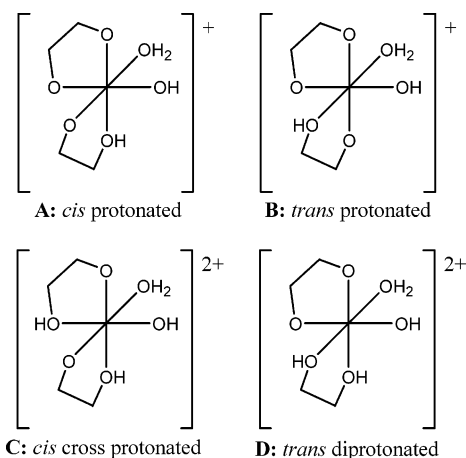
Figure 3. Pictographic representation of protonated species studied (glycol is used as an example).

quantities, namely, oxidation state, ligand types, and orientation of the ligands on the central rhenium atom. Analysis of this data will hopefully point us in the right direction with regard to improved design of future catalysts, or potentially yield insight for unrelated chemistries.

Computational Methods

Quantum mechanical computations were performed by using the B3LYP density functional. This functional is a combination of the hybrid three-parameter Becke exchange functional (B3)[12] and the Lee−Yang−Parr correlation functional (LYP).[13] The basis sets used for rhenium were the core-valence effective core potential of Hay and Wadt,[14] while the Pople-style 6-31G**[15] basis set was utilized for all other atoms. Since some reactions include negatively charged species, the effects of diffuse functions were included by computing single-point energies with the 6-31G**++ basis set. Final reported enthalpies were computed as follows:

$$H = E_{SCF}^{GP} + E_{ZPVE}^{GP} + E_{tr}^{GP} + E_{rot}^{GP} + E_{vib}^{GP} + E_{solv} \quad (1)$$

Note that E_{SCF}^{GP} is the single-point energy computed with diffuse functions at the previously optimized geometry, according to the convention B3LYP/(6-31G**++)//B3LYP/6-31G**.

All calculations were corrected for the effect of solvent interactions by using the polarizable continuum model (PCM) of solvation.[16,17] We solvated with water, which has a dielectric constant of 80.37 and a probe radius of 1.40 Å. All calculations were computed with a combination of the Jaguar 6.0 and Jaguar 6.5[18] computational packages.

The ground spin state of all reference molecules was checked, and all Re(III) species were triplets (consistent with d^4 metals). We explored the possibility of spin crossings, particularly for oxidative addition intermediates [which are formally Re(V)] and found that all reactions that started as Re(III) maintained the triplet spin state throughout the reaction. All reactions starting from the Re(V) reference were singlets.

The nature of all stationary points was confirmed with a normal-mode analysis; namely, minima had zero imaginary frequencies and transition states had one. The vibrational frequencies were used

(12) Becke, A. D. *J. Chem. Phys.* **1993**, *98*, 5648.
(13) Lee, C.; Yang, W.; Parr, R. G. *Phys. Rev. B* **1988**, *37*, 785.
(14) Hay, P. J.; Wadt, W. R. *J. Chem. Phys.* **1985**, *82*, 299.
(15) Krishnan, R.; Binkley, J. S.; Seeger, R.; Pople, J. A. *J. Chem. Phys.* **1980**, *72*, 650.
(16) Tannor, D. J.; Marten, B.; Murphy, R.; Friesner, R. A.; Sitkoff, D.; Nicholls, A.; Ringnalda, M.; Goddard, W. A.; Honig, B. *J. Am. Chem. Soc.* **1994**, *116*, 11775.
(17) Marten, B.; Kim, K.; Cortis, C.; Friesner, R. A.; Murphy, R.; Ringnalda, M.; Sitkoff, D.; Honig, B. *J. Phys. Chem.* **1996**, *100*, 9098.
(18) *Jaguar 6.0*; J. Schrodinger, LLC: Portland, OR, 2005.

to compute the zero-point correction. The total enthalpies were computed for each stationary point and used for relative enthalpy calculations (at 298.15 K).

No free energy calculations have been included in this report, due to the difficulty in accurately predicting the changes in the entropy of the translational and rotation entropy of the librational modes as molecular complexes are associated or dissociated. We expect that these entropy changes will be systematic and thus will not affect the general trends discussed here.

Results

Methane Activation. Table 1 highlights the enthalpic data, broken down by oxidation state, for the species listed in Scheme 1. The first key observation is that QMRP prototyping criteria one and two are each met only once, and no species meets both simultaneously. While the immediate conclusion is that bidentate oxygenated ligands in combination with Re(III) or Re(V) are not good systems for methane activation, the underlying causes for this are less clear and need to be further explored.

With regard to oxidation state, for the initial methane activation (namely, formation of **4**) the Re(V) species come closer to satisfying the thermodynamic criterion, i.e., that the thermodynamics for formation of $(L_1)(L_2)Re(OH_2)(CH_3)$ species is less than 10 kcal mol^{-1} endothermic. However, every single Re(III) species has a lower barrier (always metathesis) than their Re(V) counterparts. Furthermore, of the systems we find to be most promising, we observe that acac is included in every single one (even the Re(V) cases), suggesting that acac is particularly suitable to this kind of chemistry. The system with the lowest barrier was *trans* (acac)(cat)Re(OH)(OH$_2$)$^-$ with a metathesis barrier of 34.5 kcal mol^{-1}, although the other Re(III) systems have barriers that are within 2.5 kcal mol^{-1} of the best case. Oxidative addition intermediates were either higher in enthalpy than the metathesis transition state or altogether unstable, as seen in some Re(V) species, in which methane would dissociate. Thus, the favored pathway for C−H activation for all 13 species was metathesis.

When exploring the unique characteristics of individual ligands, it was observed that when paired with the acac ligand, catechol and glycol are mostly interchangeable. Relative enthalpies of (acac)(cat) and the comparable (acac)(gly) species are almost always within 3 kcal mol^{-1} of each other (within the expected accuracy range of the B3LYP/LACVP/6-31G** calculations), and the few larger differences are all within 4.1 kcal mol^{-1}. However, when (cat)$_2$ is compared to (cat)(gly)[*cis* or *trans*], deviations of over 6 kcal mol^{-1} can be observed for **9** and **12**. However, there is a very pronounced, and systematic, difference between the relative enthalpies of the *cis* and *trans* isomers when acac is one of the ligands. In almost every case the *trans* species is lower in enthalpy, in the case of [(acac)-(cat)Re(OH$_2$)(CH$_3$)]$^+$ by as much as 13.4 kcal mol^{-1}.

We also note that the enthalpy of **5** (the oxidative addition TS) is significantly lower in enthalpy than **7** (the reductive elimination TS). This suggests that if the barrier for reductive elimination could be lowered, this could eventually become a viable pathway. In the meantime, however, the metathesis pathway is preferred.

The second activation of methane with the $(L_1)(L_2)Re(OH_2)$-(CH$_3$) species (the reaction of **8** with CH$_4$), however, never proceeds via metathesis (metathesis mechanisms were explored, but none were found). Instead, the Re(III) species exhibits oxidative addition/reductive elimination exclusively. The lowest enthalpy Re(III) oxidative addition intermediate is *trans* (acac)-(cat)Re(CH$_3$)(H)(CH$_3$), at 28.8 kcal mol^{-1}.

Table 1. Relative Enthalpies (kcal mol^{-1}) of Key Intermediates and Transition States Associated with Methane Activation[a]

	Re(OH)(OH$_2$) (1)	meta TS (3)	Re(OH$_2$)(CH$_3$) (4)	OA_TS (5)	Re(OH)(H)(CH$_3$) (6)	RE_TS (7)	CH$_3$ OHM TS (9)	Re(CH$_3$)(H)(CH$_3$) (12)
Re(III)								
(acac)$_2$	**0.0**	**38.7**	**15.4**	28.1	27.1	46.7	N/A[b]	37.8
(acac)(cat)[−,c][c]	**0.0**	**36.8**	**20.7**	20.5	20.4	44.6	N/A	32.0
(acac)(cat)[−,t]	**0.0**	**34.5**	**16.3**	22.1	14.6	37.8	N/A	28.8
(acac)(gly)[−,c]	**0.0**	**36.7**	**23.3**	22.2	21.0	45.2	N/A	34.4
(acac)(gly)[−,t]	**0.0**	**36.5**	**18.5**	24.3	16.9	41.2	N/A	31.5
Re(V)								
(acac)(cat)[+,c]	**0.0**	**51.2**	**23.1**	N/C[d]	N/A	N/C	59.6	52.6
(acac)(cat)[+,t]	**0.0**	**45.4**	**9.7**	N/C	N/A	N/C	55.7	48.7
(acac)(gly)[+,c]	**0.0**	**50.5**	**19.0**	N/C	N/A	N/C	67.1	N/A
(acac)(gly)[+,t]	**0.0**	**42.1**	**11.9**	N/C	45.3	N/C	58.2	N/A
(cat)$_2$	**0.0**	**39.0**	**11.4**	N/C	32.5	N/C	49.4	37.9
(cat)(gly)[c]	**0.0**	**41.4**	**10.5**	N/C	37.6	N/C	56.1	44.0
(cat)(gly)[t]	**0.0**	**43.8**	**11.8**	N/C	N/A	N/C	57.9	45.9
(gly)$_2$	**0.0**	**41.9**	**12.6**	N/C	38.0	N/C	55.0	43.7

[a] In every case the favored primary activation is through the metathesis transition state (**3**). The components of this key activation are bolded. [b] N/A indicates that no stationary point associated with this structure was found, most likely due its being very high in enthalpy. [c] The first entry in the brackets indicates the charge of the species (if charged), while the second entry indicates *cis* or *trans* conformer. [d] Re(V) oxidative addition and reductive elimination transition states from the reference Re(OH)(OH$_2$) were not computed due to the relative high enthalpy of the oxidative addition intermediate.
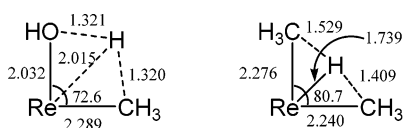
Metathesis Transition State **3**   OHM Transition State **9**

Figure 4. Key bond lengths, in Å, for the *cis* [(acac)(cat)Re(OH)(H)(CH$_3$)]$^{‡+}$ metathesis transition state and the *cis* [(acac)(cat)Re(CH$_3$)(H)(CH$_3$)]$^{‡+}$ OHM transition state.

While the Re(V) species often have a stable oxidative addition intermediate, they can also react by means of oxidative hydrogen migration. Figure 4 highlights the comparison between the *cis* [(acac)(cat)Re(OH)(H)(CH$_3$)]$^{‡+}$ metathesis transition state and the *cis* [(acac)(cat)Re(CH$_3$)(H)(CH$_3$)]$^{‡+}$ OHM transition state [no (L$_1$)(L$_2$)Re(OH)(H)(CH$_3$)‡ OHM transition states were ever observed, so we instead use (acac)(cat)Re(CH$_3$)(H)(CH$_3$)$^{‡+}$ for comparison]. The metathesis transition state is the conventional

concerted, four-membered ring transition state. The C−H bond stretches while the O−H bond forms. The OHM transition state is very different: the C−H bond is essentially completely broken and a Re−H bond is formed. The Re−H distances in the metathesis and OHM transition states are thus very different, 2.015 versus 1.739 Å (this trend is systematically present in all explored species).

Intriguingly, previous work[3,11] indicated that OHM and oxidative addition were mutually exclusive, in contradiction to the present results. However, there appears to be a substantial redistribution of the ligand framework when going from the intermediate to the OHM transition state, which would make the orbital environment of the metal dramatically different. Illustrated in Figure 5 we show the Re(V) intermediate and the OHM TS for the (gly)$_2$Re case. It can clearly be seen that the geometries of the two putative Re(V) species are very different; in the intermediate the ligand system is very distorted from the
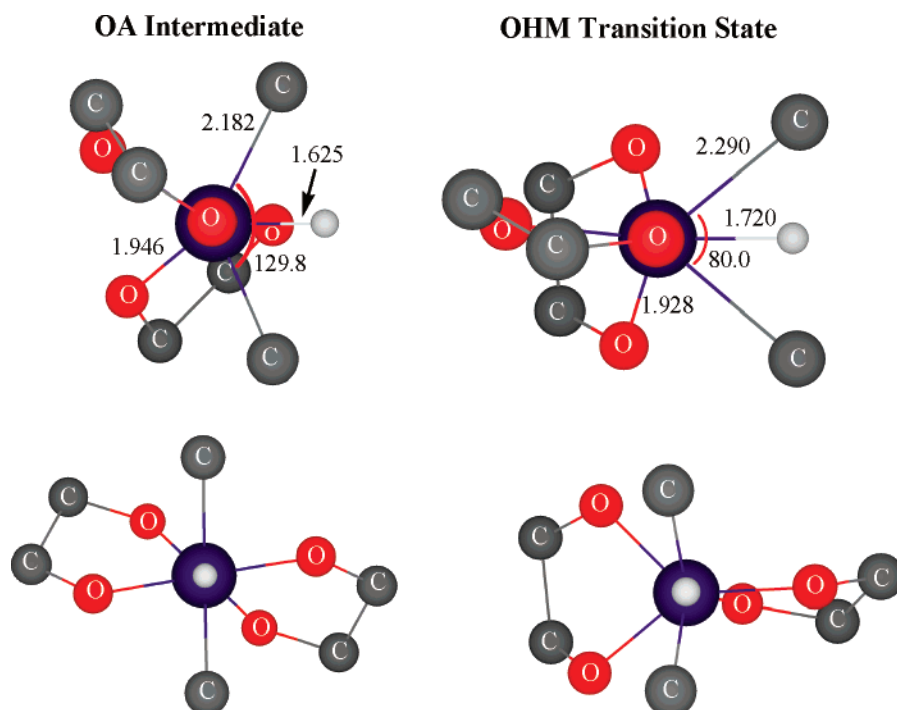
OA Intermediate   **OHM Transition State**

Figure 5. Geometrical configurations of secondary OA intermediate and OHM transition state for the (gly)$_2$Re system. The spectator hydrogens have been removed for clarity. A few key bond distances (Å) and bond angles (deg) are shown. Note the dramatic conformational change the glycols make. Two different configurations are presented to clarify the extent of geometrical perturbation between the intermediate and the transition state.

Table 2. Enthalpies (kcal mol⁻¹) of Protonated Species Relative to $L_1L_2Re(OH)(OH_2)$, with H_3O^+ [a]

	protonation
Re(III)	
(acac)$_2$	−19.9
(acac)(cat)[−,c][b]	−20.3
(acac)(cat)[−,t]	−23.5
(acac)(gly)[−,c]	−21.6
(acac)(gly)[−,t]	−24.4
Re(V)	
(acac)(cat)[+,c]	5.7
(acac)(cat)[+,t]	1.8
(acac)(gly)[+,c]	3.5
(acac)(gly)[+,t]	−5.4
(cat)$_2$	−8.3
(cat)(gly)[c]	−9.8
(cat)(gly)[t]	−8.0
(gly)$_2$	−14.3

[a] All Re(III) species are unstable in acid, but three Re(V) species are stable. [b] The first entry in the brackets indicates the charge of the species, while the second entry indicates *cis* or *trans* conformer.

original octahedral geometry, which is expected to free up space in the equatorial plane of the system and thus enable the intermediate. The TS, on the other hand, is more closely octahedral with much less distortion of the glycol moieties. Exactly how this perturbs the d-orbitals in question and how this in turn determines the presence of an intermediate or an OHM transition state is currently unclear and is under further investigation.

Acid Equilibrium Shifts. Previous work on the platinum bipyrimidine[19] system showed that activity of catalytic species could improve in highly acidic media, namely, that protonated species can react with a lower net barrier for methane activation. Before pursuing protonation of the bidentate spectator ligands, it would be beneficial to ascertain whether the ground state of the currently explored catalysts can be selectively shifted by the judicious use of acid. To simulate this, we explored the relative enthalpies for the following reactions (in which the protonated species was fully optimized):

$$(L_1)(L_2)Re(OH)(OH_2) + H_3O^+ \rightarrow$$
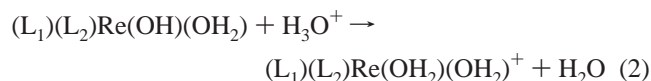$$(L_1)(L_2)Re(OH_2)(OH_2)^+ + H_2O \quad (2)$$

Table 2 shows the enthalpies for these reactions. It should be noted that these calculated enthalpies cannot be interpreted directly as acid/base equilibrium constants, since entropies are not included. However, they provide strong indicators of reactivity.

No Re(III) and only three Re(V) species were stable in 1 M H_3O^+. This does not necessarily prevent the use of these systems, as choosing the right pH might enable the desired chemistry, but it would make practical use significantly more problematic. The only stable complexes are three of the Re(V) species, all with acac, which form doubly charged species with large solvation energies. Interestingly, the *trans* (acac)(gly)Re-(V) species is not stable, while its *cis* conformer is. This is primarily a function of the relative instability of the *trans* [(acac)(gly)Re(OH)(OH$_2$)]$^+$ reference species, which is 8.9 kcal mol⁻¹ higher in enthalpy than the *cis* counterpart. Protonation of this relatively high-enthalpy reference complex is downhill.
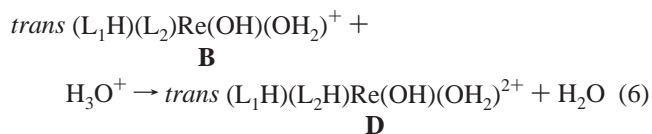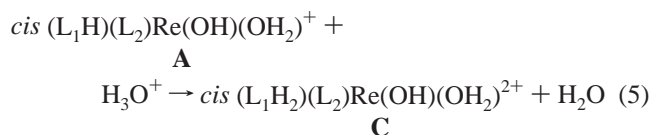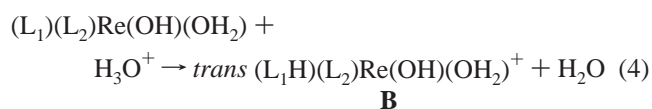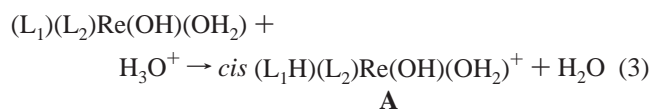
Protonated Spectator Ligands. The aforementioned work on the bipyrimidine system[19] also showed that protonation of spectator ligands of certain catalysts could lead to improved

(19) Xu, X.; Kua, J.; Periana, R. A.; Goddard, W. A., III. *Organometallics* **2003**, *22*, 2057.

Table 3. Relative Enthalpies (kcal mol⁻¹) for the Acac, Catechol, and Glycol Protonated Systems with Respect to the $(L)_2Re(OH)(OH_2)$ Reference Complex

	A	B	C	D
(Acac)$_2$Re	6.9	4.9	14.6	23.6
(cat)$_2$Re	6.9	2.5	22.5	15.1
(gly)$_2$Re[a]	−16.2	−15.1	−8.9	−11.6

[a] (gly)$_2$Re prefers protonation in the *cis* form.

reactivity. To explore this possibility in the current study, we studied the reactions 3−6, where the spectator ligands were protonated in various locations. Note that reactions 3−6 can have various conformational isomers, and the choices we considered are shown in Figure 3. We have not computed all possible protonation/deprotonation states, instead electing to study only representative choices. In all cases, complete optimizations of protonated species were performed for enthalpy determination.

$$(L_1)(L_2)Re(OH)(OH_2) +$$
$$H_3O^+ \rightarrow cis\ (L_1H)(L_2)Re(OH)(OH_2)^+ + H_2O \quad (3)$$
$$\mathbf{A}$$

$$(L_1)(L_2)Re(OH)(OH_2) +$$
$$H_3O^+ \rightarrow trans\ (L_1H)(L_2)Re(OH)(OH_2)^+ + H_2O \quad (4)$$
$$\mathbf{B}$$

$$cis\ (L_1H)(L_2)Re(OH)(OH_2)^+ +$$
$$\mathbf{A}$$
$$H_3O^+ \rightarrow cis\ (L_1H_2)(L_2)Re(OH)(OH_2)^{2+} + H_2O \quad (5)$$
$$\mathbf{C}$$

$$trans\ (L_1H)(L_2)Re(OH)(OH_2)^+ +$$
$$\mathbf{B}$$
$$H_3O^+ \rightarrow trans\ (L_1H)(L_2H)Re(OH)(OH_2)^{2+} + H_2O \quad (6)$$
$$\mathbf{D}$$

For the protonated ligands we considered a subset of the intermediates and transition states, namely, **1**, **3**, **4**, and **6**. The subset was chosen to quickly ascertain if there was a marked change compared to the neutral species and, in addition, if either of the QMRP criteria was met by the protonated reference species. Table 3 highlights the protonation enthalpies of the various protonated species, and Table 4 lists the enthalpies associated with methane activation for these protonated catalysts.

For the (acac)$_2$ and (cat)$_2$ species the protonated forms are uphill in enthalpy (4.9 kcal mol⁻¹ for acac and 2.5 kcal mol⁻¹ for catechol), but low enough that non-negligible amounts of the protonated forms would be present in an acidic environment. Glycol, however, is strikingly different. Both the *trans* and *cis* monoprotonated forms are downhill in enthalpy by over 15 kcal mol⁻¹. This does not appear to be a solvation issue, as gas-phase protonated glycol species are over 20 kcal mol⁻¹ more stable than their catechol counterparts; namely, the gas-phase protonation enthalpy is −45 kcal mol⁻¹ for *trans* protonated catechol and −66 kcal mol⁻¹ for the glycol analogue. Most likely, protonating catechol destroys the quasi-aromaticity of the five-membered ring formed by the metal and the catechol linkage, which renders the protonation unfavorable. There is no such issue for glycol, leading to a more basic character.

We see a similar trend for the diprotonated species: the acac and catechol species are very high in enthalpy, but the glycol species, while only slightly higher than the monoprotonated forms, are still below the neutral species. The overall reactivity

Table 4. Relative Enthalpies (in kcal mol⁻¹) of Key Intermediates and Transition States Associated with Methane Activation for Protonated Species[a]

	$Re(OH)(OH_2)$ (**1**)	Meta TS (**3**)	$Re(OH_2)(CH_3)$ (**4**)	$Re(OH)(H)(CH_3)$ (**6**)
(acac)₂				
1 (nonprotonated)	0.0	38.7	15.4	27.1
A	0.0	37.8	10.6	26.8
B	0.0	38.4	9.0	25.8
C	0.0	45.7	16.9	33.9
D	0.0	39.5	5.5	N/A[b]
(cat)₂				
1 (nonprotonated)	0.0	39.0	11.4	32.5
A	0.0	42.5	7.2	48.1
B	0.0	46.4	16.6	33.5
C	0.0	47.4	1.8	N/A
D	0.0	50.2	16.8	N/A
(gly)₂				
1 (nonprotonated)	0.0	41.9	12.6	38.0
A	0.0	44.4	12.0	50.9
B	0.0	48.2	18.7	N/A
C	0.0	47.2	7.5	44.9
D	0.0	47.0	13.0	59.5

[a] The nonprotonated species is included for reference. Thus, the protonated forms do not produce more reactive reference species. [b] We were unable to find the structure for this species.

Mulliken Charge vs. Metathesis Barrier
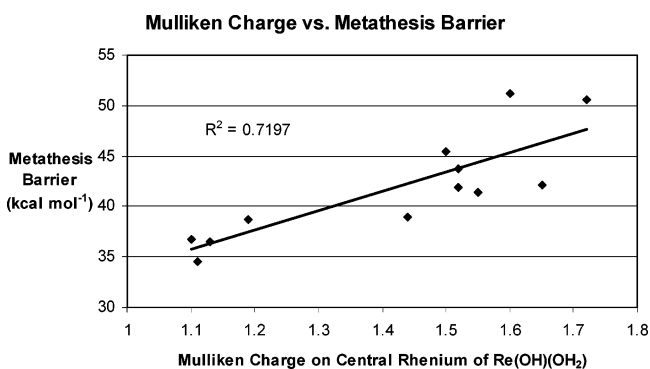
Figure 6. Plot of metathesis barrier (kcal mol⁻¹) versus Mulliken charge on the central rhenium atom of $Re(OH)(OH_2)$.

with methane does not improve for the protonated species; indeed, in most cases the barriers increase. While for several cases the thermodynamic criterion is met, in only one case is the activation barrier of a protonated form below the neutral case [(acac)₂ *cis* protonated], and only by 0.9 kcal mol⁻¹.

Discussion

The previous sections have outlined some of the trends associated with methane activation by oxygenated rhenium complexes. The main observation is that methane activation proceeds with a lower barrier when starting with lower formal oxidation states. When considering oxidative addition as a pathway, this is intuitive. A Re(V) reference molecule would have to go through a high-enthalpy Re(VII) intermediate, which would be unfavorable. This is also the reason why the second activation can proceed through an OHM mechanism for Re(V); the alternative oxidative addition is too high in enthalpy. For Re(III), oxidative addition is not so high in enthalpy, and thus it remains a viable pathway.

However, it is less clear why Re(III) also has a lower barrier for metathesis than reductive elimination, as metathesis does not increase the formal oxidation state. It seems the metathesis barriers are fundamentally linked to the electron density on the central rhenium. Consider Figure 6, which plots the Mulliken charge on the rhenium versus the metathesis barrier. While the trend is not strictly linear, a clear relationship between electron

Table 5. Relative Enthalpy of 2, with Subsequent Metathesis Barrier in Parentheses, in kcal mol⁻¹ [a]

	Re(III)	Re(V)
(acac)(cat)[*cis*]	5.7(36.8)	13.8(51.2)
(acac)(cat)[*trans*]	2.7(34.5)	11.3(45.4)
(acac)(gly)[*cis*]	4.9(36.7)	12.6(50.5)
(acac)(gly)[*trans*]	2.0(36.5)	3.7(42.1)

[a] These numbers represent the relative lability of the water ligands.
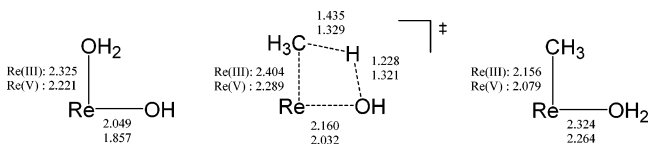
Figure 7. Key bond distances in species **1**, **3**, and **4** (Å) for *cis* (acac)(cat)Re(OH)(OH₂) Re(III) and Re(V) species.

density on the metal and activation barrier is present, with more electron density on the metal leading to a decreased metathesis activation barrier. Indeed, preliminary calculations indicate that the metathesis activation barriers and Mulliken charges on the central rhenium for various oxidation states are correlated [for example, for (acac)₂Re(OH)(OH₂) we calculate Re(II)[−1] 34.4 kcal mol⁻¹ (Mulliken charge on Re, 0.94), Re(III)[neutral] 38.7 kcal mol⁻¹ (Mulliken charge on Re, 1.19), and Re(IV)[+1] 52.8 kcal mol⁻¹ (Mulliken charge on Re 1.52)]. As this is still a preliminary study, we do not yet claim that the Re(II) species is best for methane activation, merely indicating that decreasing the formal oxidation state on the central rhenium can lower significantly the activation barrier of methane. Clearly, increasing electron density on the central rhenium leads to lower metathesis activation barriers.

To elucidate the origins of this behavior, we turned our focus onto the systems with the acac ligand. These complexes have the advantage of allowing us to explore two systems that have exactly the same ligand framework, but differ only in the formal oxidation state of the metal, simply by changing the formal charge of the complex.

Changes in reactivity for a single mechanistic step can be caused by either a change in ground state enthalpy or transition state enthalpy. To decouple these effects, we first considered the lability of the water ligand (that is, the relative enthalpy of $(L_1)(L_2)Re(OH)$, **2**, plus free H₂O) to ascertain whether the enthalpy of the ground state changes between the various systems. Table 5 lists these enthalpies for select Re(III) and Re(V) systems, along with the subsequent metathesis barrier. Note the higher lability for the Re(III) species. Key bond lengths of the Re(III)/Re(V) (acac)(cat)Re(OH)(OH₂) species are also good indicators of bond strength and concomitant lability and are shown in Figure 7. This shows bond lengths consistent with the relative enthalpies of the transition state (**3**) and activated product (**4**) (the structural data for the other acac species are consistent with the trends shown in Figure 7). The Re(III) species forms longer (and thus weaker) Re−O bonds, leading to an increased lability of the water in Re(III) species. The improved lability of water on Re(III) lowers the barrier of methane activation for Re(III) relative to Re(V).

The other key factor in the magnitude of the barriers is the relative enthalpy of the transition state. The Re(V) species have larger barriers as a direct result of the increased Re−O bond strength, relative to Re(III). Also, a more immediately accessible measure of the bond strength is the Re−O bond length, as shown in Table 6, where Re−O bond distances for multiple oxidation states of rhenium are listed. Shorter bonds are directly related

Table 6. Re—O and Re—C Bond Distances (Å) for Multiple Oxidation States of Rhenium

oxidation state	Re—O bond length	Re—C bond length
Re(I)	2.277 [(en)$_2$Re(OH)(OH$_2$)]	2.151 [(en)$_2$Re(CH$_3$)(OH$_2$)]
Re(III)	2.009 [(acac)$_2$Re(OH)(OH$_2$)]	2.131 [(acac)$_2$Re(CH$_3$)(OH$_2$)]
Re(V)	1.925 [(gly)$_2$Re(OH)(OH$_2$)]	2.108 [(gly)$_2$Re(CH$_3$)(OH$_2$)]
Re(VII)	1.873 [HReO$_4$]	2.086 [CH$_3$ReO$_3$]

to increased bond strength,[20] and it is thus clear from Table 6 that the bond strengths increase with the increased oxidation state. In addition to the effect of a smaller atom radius in Re(V) as compared to Re(III), this is most likely due to the increased availability of unoccupied metal d-orbitals for accepting the oxygen's lone pairs in the higher oxidation states, resulting in stronger bonds.

Thus, to reach the transition state, the Re(V) complexes must break a significantly stronger bond, which translates into a higher barrier. Another way to look at this phenomenon is the amount of bond stretching required to reach the transition state. Consider the transition state in Figure 7, and note that the Re—O bond is more stretched (relative to the reactant **1**) for Re(V) than for Re(III) [0.175 Å stretch for Re(V) and 0.111 Å stretch for Re-(III)]. Note how the R—C bonds do not change as appreciably as the Re—O bonds, since carbon does not have any lone pairs to donate.

The relative disparities between the *cis* and *trans* isomers of the various acac species is primarily a *trans* influence. The acac ligand is a mixed L—X type ligand (see, for example, ref 11), more weakly bound to the metal than the true X—X type catechol and glycol ligands. OH (which bonds more tightly to Re than OH$_2$) prefers to be *trans* to the weaker Re—acac bond. This is shown in the thermodynamics, in which the *trans* (acac)-(X)Re(OH)(OH$_2$) (X = cat or gly) is always higher in enthalpy than the *cis* analogue. The activation barriers for *trans* species are thus lowered by ground state destabilization of the (L$_1$)-(L$_2$)Re(OH)(OH$_2$) reference complex. Furthermore, the distinction between the catechol and glycol ligands is very small, with the only significant difference between them being the basicity of the ligand oxygens (glycol is easily protonated, while catechol is not). This observation suggests that there is no correlation between the energy of the occupied d-orbitals (which would be influenced by the quasi-aromatic ground state) and the OH$_2$ binding enthalpy.

Note, however, that even though the *cis* and *trans* (acac)-(gly)Re(III) species have dramatically different water labilities, the activation barriers are almost identical. The implication is thus that while ground state stabilization appears to be important, the barrier heights are dependent on transition state stabilization as well.

The goal of the present work was to determine if oxygenated ligands could make viable methane activation ligands, and the immediate answer is no. However, our analysis has led us to several concepts to keep in mind when designing a rhenium-based methane activation catalyst. First and foremost, to improve catalytic reactivity with methane, increase electron density on the central metal. Increasing electron density on the central metal weakens the Re—O bond, making the water more labile, while also lowering the barrier for proton transfer from methane. In general this can be done by formally lowering the oxidation state of the metal, but also by using more electron-donating ligands. Additionally, catalysts with oxygenated ligands should

be utilized in neutral environments, as both acid and base shift equilibrium away from the reference species (L$_1$)(L$_2$)Re(OH)-(OH$_2$) to less reactive protonated and deprotonated forms. These concepts will be used to guide further exploration of rhenium-based systems for methane activation.

Summary

We have explored the reactivities of several Re(III) and Re-(V) systems, formed with bidentate oxygenated ligands, with methane under several different circumstances. Unfortunately, none of the model systems are predicted to be viable catalysts for methane activation, generally failing both the thermodynamic and kinetic criteria for potential use in almost all cases and never simultaneously satisfying both. The best potential catalyst was the *trans* (acac)(cat)Re(III) system with a barrier of 34.5 kcal mol^{-1}. Protonation of the oxygenated ligands occasionally helped potential catalysts satisfy the thermodynamic criterion, but never the kinetic one, and as it seems not to be a general trend, it is unlikely to help in other oxygen-based systems.

The majority of the reference species of the form (L$_1$)(L$_2$)-Re(OH)(OH$_2$) are not the ground state in acidic environment, as protonation of the M—OH using 1 M H$_3$O$^+$ is usually downhill in enthalpy. The lone exceptions to facile protonation are both (acac)(cat) complexes and the *cis* (acac)(gly) Re(V) species.

The most significant trend to note is the importance of electron density on the central metal atom. Increased electron density on the metal tends to lower barriers for methane activation. Considering the barriers/Mulliken charges on the two (acac)(cat) species, for Re(III) we have 36.8 kcal mol^{-1}/1.10 electrons, while for Re(V) we have 51.2 kcal mol^{-1}/1.60 electrons. To improve catalytic reactivity with methane for catalysts which use OH to capture a proton from CH$_4$, increase electron density on the central metal. Increasing electron density on the central metal weakens the Re—O bond, making the leaving group more labile and making it easier for the OH to accept a proton. Decreased electron density can be accomplished by formally lowering the oxidation state of the complex or through the use of more electron-donating ligands. In an asymmetric complex (L$_1$ ≠ L$_2$), placement of the labile ligand (OH$_2$ in the present work) in the reference molecule is also important. If it can be placed *trans* to the more weakly bound of the two ligands, ground state destabilization will lower activation barriers. Finally the difference in reactivity between catechol and glycol species was minimal, implying the overall rigidity of the oxygenated ligand is not important, rather how it effects the electronic environment of the central metal.

Conclusions

The current generation of oxygenated ligands does not provide viable choices for activation of methane. Increased electron density on the central rhenium is the key to improved activation, improving the lability of the necessary leaving group and lowering the barrier to proton transfer from methane. Thus, alternate ligand systems, primarily more electron donating (possibly nitrogen-, phosphorus-, or sulfur-based ligands), are currently under investigation.

Supporting Information Available: This material is available free of charge via the Internet at http://pubs.acs.org.

OM0606901

(20) Haaland, A.; Green, J. C.; McGrady, G. S.; Downs, A. J.; Gullo, E.; Lyall, M. J.; Timberlake, J.; Tutukin, A. V.; Volden, H. V.; Østby, K. *Dalton Trans.* **2003**, 4356.